Implanted muon spin spectroscopy on 2-O-adamantane: A model system that mimics the liquid⟶glasslike transitions

M. Romanini, J.Ll Tamarit, L.C. Pardo
Grup de Caracterizacio de Materials, Departament de Fisica,
ETSEIB, Universitat Politecnica de Catalunya, Diagonal 647, 08028 Barcelona, Catalonia, Spain

F.J. Bermejo, R. Fernandez-Perea
Instituto de Estructura de la Materia,Consejo Superior de Investigaciones Cientificas,
Serrano 123, E-20886 Madrid, Spain

F.L. Pratt
ISIS Neutron and Muon Source, STFC Rutherford Appleton Laboratory,
Chilton, Didcot, Oxfordshire, OX11, 0QX, United Kingdom

December 2, 2016

Abstract

The transition taking place between two metastable phases in 2-O-adamantane, namely the $Fm\bar{3}m$ cubic, rotator phase and the lower temperature $P2_1/c, Z = 4$ substitutionally disordered crystal is studied by means of muon spin rotation and relaxation techniques. Measurements carried out under zero, weak transverse and longitudinal fields reveal a temperature dependence of the relaxation parameters strikingly similar to those exhibited by structural glass⟶liquid transitions (Bermejo et al. Phys. Rev. B 70, 214202 (2004); Cabrillo et al. Phys. Rev. B 67, 184201 (2003)). The observed behaviour manifests itself as a square root singularity in the relaxation rates pointing towards some critical temperature which for amorphous systems is located some tens of degrees above that shown as the characteristic transition temperature if studied by thermodynamic means. The implications of such findings in the context of current theoretical approaches concerning the canonical liquid-glass transition are discussed.

Keywords

disordered systems, muon spin rotation, relaxation and resonance

1 Introduction

The interest in the study of molecular materials showing some sort of disorder in one degree of freedom, while retaining ordered crystal structures for the rest, has reawakened in recent decades. This is mostly because of the possibilities such materials offer as model systems to extend our understanding of the properties exhibited by structurally disordered matter, but also due to some potential applications that were recently envisaged [1]. Materials prepared into such states are known to exhibit at low temperatures thermal, acoustic and dielectric properties which significantly differ from those shown by the same substances if prepared within their fully ordered, crystalline ground states. However, after some decades of extensive studies, our understanding of most features commonly ascribed to *glassy dynamics* mostly relies on phenomenological concepts [2], many of which have been developed as tools to quantitatively describe the physical state of simpler systems such as substitutional defects in alkali halides [3] as well as mixed halide crystals [4]. Such model systems display a full range of phenomena well understood microscopically, which go from tunneling motions of a single atom to interacting tuneling states in cases

with large concentrations of substitutional defects, which were shown to exhibit fully developed *glassy behaviour* .

The phenomenology considered to be the distinctive signature of the *glassy state* is nowadays known to be shared by a wide number of systems [5] which go from partially ordered crystals to concentrated colloidal solutions, cold compressed crystals or idealized toy-models [6]. Several of such studies on partially ordered crystals have shown [7] these materials to exhibit phenomena remarkably close to those shown by the same material if prepared as a fully disordered substance. As a further step, recent additions to the literature [8] include incommensurately modulated crystals which exhibit at low temperatures similar features to those shown by amorphous materials, and are found to originate from the gapped phase and amplitude modes of the incommensurate crystal structure.

Here we report on issues pertaining to a transition between disordered crystal states on the adamantane derivative 2-O-adamantane ($C_{10}H_{14}O$, also referred to as 2-adamantanone), which retains significant analogies with the canonical *liquid* $\longrightarrow$ *glass* transition . The material, which can be prepared into different phases when cooling down the liquid from 557 K, exhibits a rich polymorphism at ambient pressure [9–13]. In fact, freezing the stable liquid leads to a rotator-phase (RP) or plastic-crystal state [9] where individual molecules having C_{2v} point group symmetry sit at the nodes of a face-centered $Fm\bar{3}m$ cubic lattice and execute large amplitude, quasi-isotropic orientational excursions involving jumps between six possible orientations of the C=O group along the six fourfold crystal axes as well as $\pi/2$ flops about the C=O axis. Further cooling, below 178 K leads to a metastable, $P2_1c, Z = 4$ monoclinic unit cell where statistical disorder is manifest by the site occupancy of the oxygen atom which may lie in three different crystallographic sites with fractional occupancies of 25%, 25% and 50%, here referred to as substitutionally-disordered phase (SDP). A true crystalline, fully-ordered ground state is only attained after repeated thermal cycles comprising the transition temperatures $\simeq$ 100 K - 220 K leading to repeated $RP \rightleftharpoons SDP$ interconversions.

Relatively fast molecular rotations were reported for adamantane derivatives and adamantanone in particular [14–16], which show that in contrast to rapid isotropic rotational reorientations found for the former in liquid or even within the solid at 294 K where rotational diffusion constants still are of the order of $10^{10}\mathrm{rad}^2\mathrm{s}^{-1}$, rather extreme anisotropic reorientations were found for the latter. Interestingly, while the isolated molecule closely behaves as a symmetric top with calculated rotational constants of 1678.6 MHz, 1201.5 MHz, and 1191.6 MHz, the principal values of the rotational diffusion tensor as determined from NMR spectroscopy in the liquid phase [14] unveil a marked motional anisotropy with a proportion 1:2:24, where the faster rate corresponds to reorientations along an axis passing through the C=O bond.

The interest in carrying out a detailed study on the dynamics of the $SDP \longrightarrow RP$ transition stems from findings previously reported by Brand *et al.* [10] and recently confirmed by Romanini *at al.* [11] which report on fairly well defined *glassy dynamics* features within the SDP phase by means of broadband dielectric spectroscopy, which were tentatively assigned to interconversions between the statistically disordered sites. Such findings contrast with previous spectroscopic results [17] which overlooked such microscopic motions most probably due to their available time windows. The presence of such motions thus suggests the non-ergodic nature of the SDP phase below a certain glass transition temperature [11] and therefore constitutes a valid analogue of a glass, since the former state is attained by virtue of the continuous slow down of the nearly free rotations present in the RP crystal.

The present paper reports on results from measurements about the $SDP \longrightarrow RP$ transition carried out by means of a spectroscopic technique able to detect single-particle motions taking place over a quite broad range of characteristic times ($10^{-12} - 10^{-4}$ s) . In fact, here we show that spin relaxation spectroscopy with implanted positive muons provides a unique means to monitor the phase transformation referred to above. Previous studies on canonical *glass* $\longrightarrow$ *liquid* transitions [18, 19] have shown that measurements of the polarization function of the muon decay in weak transverse magnetic fields display unambiguous signatures of critical behaviour at temperatures somewhat above those signaling the thermodynamic glass transition, namely at the onset of stochastic molecular motions. The temperature dependence of transverse relaxation rates and amplitudes is found to provide sound evidence for the existence of a critical temperature T_c as predicted by kinetic theories of the glass transition.

2 Materials and methods

The technique here employed consists in the measurement of the temperature and applied field dependences of the spin relaxation characteristics of implanted positive muons onto a sample of 2-O-adamantane previously prepared within the crystal state of interest. Because of the small muon mass, once the incoming muon reaches the end of the ionization track and gets fully thermalized, its motions once implanted at specific sites of the crystal structure will be driven by the excitations of its microscopic environment to which it is strongly coupled. The latter depends upon known radiochemical details pertaining to the fate of the implanted muon.

The measurements were carried out using the ARGUS muon spin relaxation (μSR) spectrometer hosted by the ISIS pulsed source. The instrument was set up in a standard μSR configuration. The incoming beam was collimated down to a spot of 30 mm and spectra were left to accumulate some 10 million events. The sample was purchased from Aldrich Chemical with a stated purity of 99 % and used as received. Specimens for the muon experiments were prepared by enclosing some 0.8 g of the pristine powdered material within a 3 cm $\times$ 3 cm silver foil packet. Spectra under longitudinal (LF) and transverse (TF) fields were then measured from 20 K up to temperatures well above the $SDP \longrightarrow RP$ transition, namely 300 K. The analysis of experimental data has been carried out employing software packages specially developed at ISIS, i.e. the WIMDA [20] and MantidPlot packages [21].

3 Results

3.1 Characterization of muon sites

From the chemical nature of the sample we are dealing with, several kinds of muon species are to be expected. Some muons may remain as bare μ^+, whereas others will capture an electron, leading to formation of atomic Muonium Mu($\equiv \mu^+ e^-$). Both these species will sit within the crystal interstices and may execute diffusive or jumping motions. Both μ^+ and Mu will stick to 2-O-adamantane molecules near the Oxygen attracted by its electronegativity [22]. The final state of such a muoniated adduct may either be as a charged molecule 2-O-adamantane-Mu$^+$, closed shell in character and thus diamagnetic or rather a neutral 2-O-adamantane-Mu, which will probably have some distribution of unpaired spin density and is thus paramagnetic. Further implantation sites leading to the formation of adamantanyl radicals [23, 24] are deemed to be far less abundant on account of the rather low chemical affinity of the known implantation sites if compared to that of the carbonyl group.

A series of calculations employing quantum chemical tools have been carried out in order to clarify the chemical fate of the implanted muons as well as the properties of the muoniated molecules. The CASTEP [25] and DALTON [26] codes have been employed for such a purpose. The geometry and some properties of isolated molecules have been first calculated either at Hartree-Fock or DFT/B3LYP levels in order to get some indications on their relative stability as well as to guess some relevant spectroscopic properties such as the values of the hyperfine coupling parameters. The obtained results show that both neutral and charged muoniated species appear to be stable enough having a difference in energies of roughly 4 eV, depending upon the computational method employed for the purpose [27].

The obtained fully relaxed molecular geometries show the muon rest place as attached to the carbonyl Oxygen, separated by a distance of 0.97 Å making a C-O-Mu bond angle of 113.3 ° with the muon staying within the C-C-O plane. Figure 1 displays the results of one calculation carried out using the CASTEP code showing the muon bonded to one of the carbonyl Oxygens.

Detailed calculations show that the muoniated molecule is a symmetric top with a ratio of its principal moments of inertia of 0.7:1:1 with 72 molecular vibrational modes with frequencies comprising 19.3 meV - 463.8 meV. The lowest vibrational frequency corresponds to a normal coordinate in which several atoms including the stuck muon execute low amplitude motions. For the temperature range of interest however, the vibrational contributions of an isolated molecule to the total molecular partition functions are of the order of 2 $\times 10^{-6}$ or below if compared to their rotational counterparts.

3.2 Properties of the muoniated radical

Previous results on the chemically related molecule acetone [28] report on data where some 53 per cent of the implanted muons end up within diamagnetic molecular environments. Such a relatively large

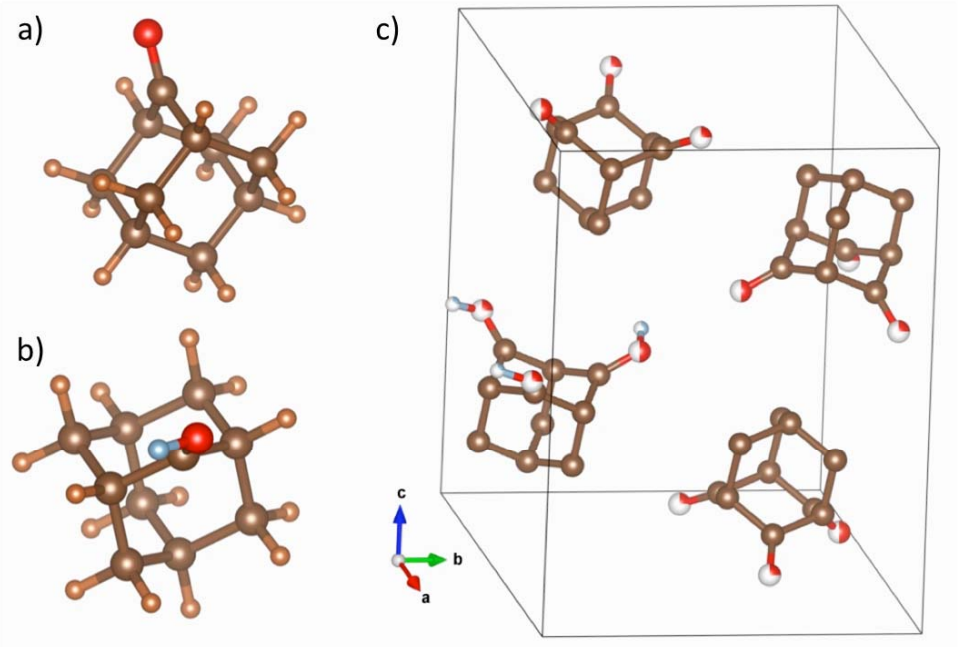

Figure 1: (a) Molecular structure of the 2-O-adamantane molecule. Oxygen is shown as a red/white sphere, carbons as brown and hydrogens as pale brown spheres. (b) Structure of the molecule following addition of μ^+ or Mu. The bonded μ^+/Mu is depicted as a pale blue/white atom-like sphere. (c) The arrangement of molecules within the $P2_1c, Z = 4$ monoclinic crystal structure showing multiple possible sites for the O (hydrogens are omitted for clarity). The colour code for the Oxygen and Mu is meant to give an indication of the fractional occupancy probabilities, that is the pale-blue and red depict occupational probabilities of a given species in such a crystal site.

diamagnetic fraction is thus thought to arise from 2-O-adamantane-Mu$^+$ cations. Following the track of such studies which mostly focus on radiochemical details, we first attempted a measurement using the technique of avoided-level-crossing (ALC) resonance for the sought 2-O-adamantane paramagnetic radical fraction. The expectancy was to find some signature of the Δ_1 resonance which corresponds to muon spin flips induced through the coupling of the Zeeman states from the anisotropic part of the muon-electron hyperfine interaction as a dip in the signal amplitude. For such an avail we took the value for the muon hyperfine coupling constant (HFCC) of the Mu adduct of acetone of 25.4±0.6 MHz at 298 K [28] on the basis of the local chemical analogy of both compounds, leading to an expected resonance centered at about 930 G. If this were proven to be the case then the onset of rotation of the C=O bond would result in the muon HFCC changing significantly. Molecular rotations would then significantly reduce the dipolar coupling between the bonded muon and nearby protons and lead to a reduction in the width and amplitude of the resonance. Initial measurements of the relaxation parameters measured under longitudinal (LF) fields up to 4 kG and a full set of temperatures both within the SDP and the RP ranges of existence did not reveal any clear signature of the presence of such a resonance in the form of a sharp dip. To clarify this apparent discrepancy, a series of computations were carried out in order to derive estimates of the hyperfine coupling constants for the 2-O-adamantane-Mu adduct. Precise details about such calculations as well as the resulting estimates for the principal values of the symmetrized (i.e. diagonal) hyperfine coupling (HFC) tensor at the muon site and the axial and non-axial dipolar anisotropy terms are given as Supplementary Material. The results show that the estimation of the isotropic HFCCs are extremely sensitive to the local molecular geometry about the muon binding site and point towards a remarkable dependence of their values upon molecular internal motions which usually vibrate at frequencies which are comparable to those of the molecular lattice modes.

In summary, our present findings suggest that the radical state shows a strong dependence upon molecular motions which may provide an interesting handle for further studies on the temperature dependence of the hyperfine coupling parameters thus leading to estimates for the relevant microscopic

correlation times. In what follows however, we will mostly rely upon data measured under transverse fields, whose interpretation is much more straightforward, taking data measured under zero field as a consistency test which is also reported on as Supplementary Material.

3.3 Transverse field studies

Let us first discuss the results pertaining to the TF setup. Such data if taken at a pulsed muon source such as ISIS will provide access to details of the dynamics of diamagnetic species alone, due to the limited frequency window for rotation signals, whereas measurements carried out under longitudinal fields will also sense the paramagnetic muonium via the time-averaged polarisation.

The spectra yield relaxation rates $\lambda_{TF}(T)$ and their corresponding amplitudes which contain information on static or *frozen-in* spatial fluctuations of the local magnetic field since they induce dephasing among the spin precession of muons located at different sites. In other words, the relaxation is also driven by a zero-frequency term $J(0)$. Such spectral density is also sampled by experiments carried out under longitudinal fields (LF) which sample the $J(\omega_0)$ spectral density of the local magnetic field fluctuations at the Larmor frequency for the muon states (or, for muonium, at various transition frequencies of the hyperfine-coupled spin states). Also, in the absence of any externally applied field, the implanted muons will precess at a frequency set by the internal fields. The physics sensed by such zero-field (ZF) experiments would be quite similar to the TF case although any contribution from paramagnetic species is to be expected. Signatures of such latter entities are in fact observed and a more detailed account is deferred to the relevant section within the Supplementary Material.

Some representative histograms showing the time evolution of the muon polarization comprising two significant temperatures within the range of interest are shown in Fig.2. As expected, measurements carried out at the lower range of temperatures show damped oscillations in their decay curves whereas those measured for temperatures above the $SDP \longrightarrow RP$ transition show small decay rates with a rather soft dependence with temperature.

The transverse field spectra can be well approximated by a damped cosine signal namely,

$$P_{TF}(t) = a_{TF} \exp\left(-\lambda_{TF} t\right) \cos\left(\omega_0 t + \phi\right) + bcgr \tag{1}$$

where ω_0 stands for the Larmor frequency corresponding to the effective field sensed at the muon site $\omega_0 = \gamma_\mu B_{eff}$, $\gamma_\mu = 2\pi \times 13.55\ kHzG^{-1}$ stands for the muon gyromagnetic ratio and B_{eff} is the field experienced at the muon site, which for a diamagnetic material is expected to be rather close to the applied external field, ϕ is a phase shift related to the detector geometry and signal timing and λ_{TF} is a relaxation rate which accounts for both the distribution of local fields and their time-dependent fluctuations. A small background term *bcgr* was left as a free parameter in a first round of spectral fits. Its value was then set to the average taken over the whole temperature range and left as a constant in subsequent fits.

A graph displaying the temperature dependence of the relaxation rate λ_{TF} and relative amplitude a_{TF} as measured for increasing temperatures under an applied transverse field of 50 G is shown in Fig.3. Both quantities show an abrupt change when the transition $SDP \longrightarrow RP$ is approached. Such features are here far more marked than those already reported for canonical $glass \longrightarrow liquid$ transitions [18, 19] and discussion of their physical relevance is deferred to the next section.

As stated above, only diamagnetic species contribute to the measured intensity at a pulsed source such as ISIS under the applied fields here employed and therefore the interpretation should be straightforward. In fact, the technique is equivalent to the measurement of free induction decays in conventional ^{1}H NMR and corresponds to precession of the muon spin at or near its Larmor frequency. In turn the much higher precession frequencies of atomic muonium can only be observed at continuous muon sources. Such measurements are sensitive to static, (i.e. time averaged) spatial disorder and therefore can be compared to the second moment of the proton NMR line, $M_2(T)$ [29] which for our sample was studied by Amoreux and others in ref [17]. The reported rigid-lattice value for the SDP is some 21 G^2 larger than that for the RP. Such a difference is also sensed by our λ_{TF} data down to 10 K. However, contrary to the NMR results which show an abrupt jump at the crystal transition and basically no dependence with temperature down to a few kelvins, our data displayed in Fig.3 do show a marked dependence with decreasing temperature. The reason behind such different results coming out from the two techniques is well established and has to deal with the rather different rates of dynamic fluctuations explorable by

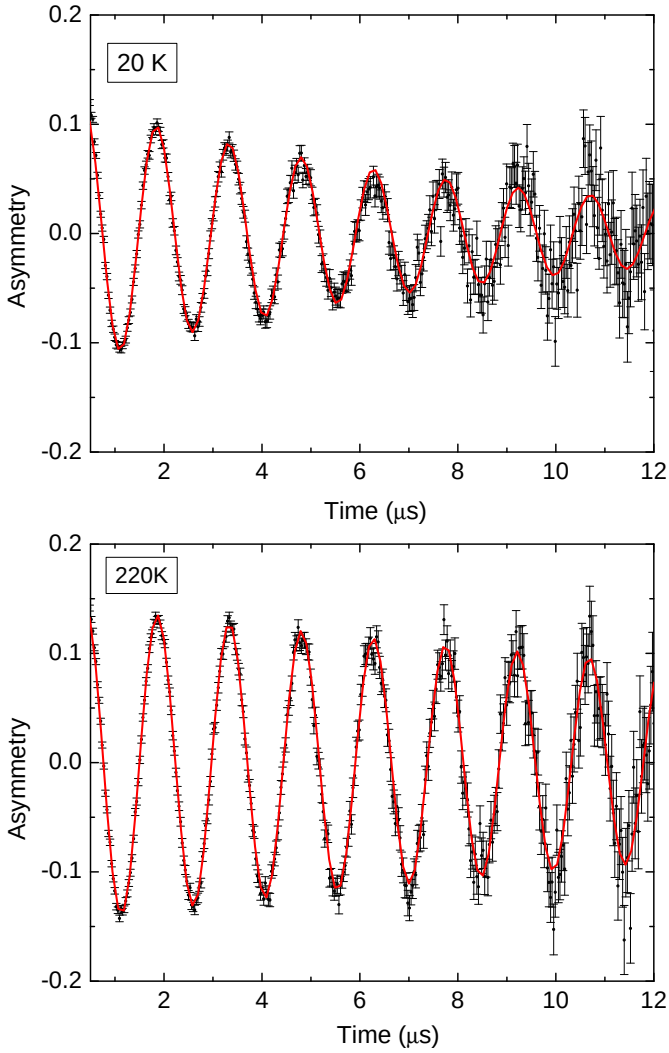

Figure 2: A sample of spectra as measured under a transverse applied field of 50 G for two temperatures corresponding to the SDP at 20 K and for the RP at 220K. The solid lines depict fits to Eqn.1.

magnetic resonance and muon spectroscopies. In fact, as it is now well established, μSR techniques are able to explore a wide range of fluctuation rates, namely 10^4Hz $- 10^{12}$Hz, whereas magnetic resonance techniques are generally restricted to explore phenomena with slower fluctuation rates within the range 10^{-2}Hz $- 10^5$H [30]. The reduction of λ_{TF} with increasing temperature is thought to arise from the onset of some molecular motions which will become rather fast within the RP state and consequently only a weak dependence of λ_{TF} with temperature is found there. As discussed below, the measured rates λ_{TF} monitor the development of a time-averaged component that parallels the behavior of the Lamb-Mössbauer (or Debye-Waller) factor which can be measured by various other spectroscopies. As shown in Figure 3 , above some 170 K, motional narrowing within the SDP crystal departs from the simple thermally activated behaviour expected for the Debye-Waller factor of a harmonic sample i.e., $\ln(\lambda(T))$ significantly departs from a straight line. The drastic reduction in relaxation rate witnessed above some 160 K thus monitors the emergence of critical dynamics leading to the phase change.

To compare the results with well defined physical quantities we have computed the rigid-lattice value

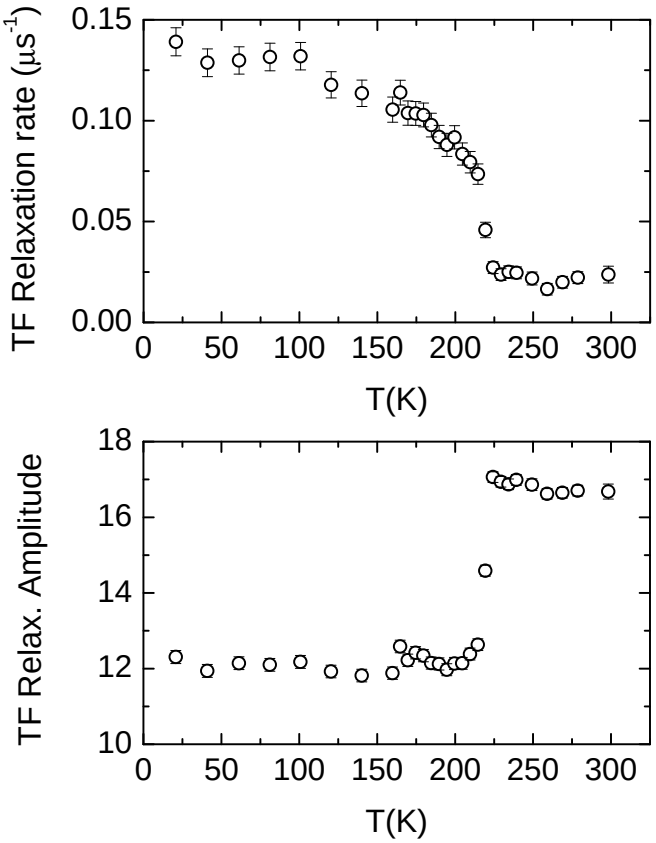

Figure 3: Temperature dependence of the observed relaxation rates (upper frame) and amplitudes (lower frame) resulting from measurements carried out under a transverse applied field of 50 G.

for a polycrystalline sample as calculated after an orientational average and reads,

$$M_{2,poly} = \frac{4I(I+1)}{15}\hbar^2\gamma_\mu^2\gamma_N^2\sum_{j=1}^{N}\frac{1}{r_j^6} \tag{2}$$

where γ_N stands for the gyromagnetic ratios of proton nuclei close to the muon site. For such a purpose a crystal structure having an implanted Mu has been evaluated by means of a DFT calculation which employed the crystallographic structure determined from diffraction experiments [9] and thus enabled the optimization of the Mu location within the 2-adamantanone-OMu adduct. The summation was run up to distances reaching 10 Å from the Mu location. The estimation was carried out using the programme developed by Goc [31] which enables the calculation of van Vleck second frequency moment [32] for materials composed of molecules which may have some internal degree of freedom. The result yielded a value of 24.9 G^2 which is to be compared with that of 22 G^2 derived from broadband NMR [17] and provides an estimation of the root-mean-squared field spread causing dephasing Δ within the static limit [33] of $\approx$ 10 G.

Dynamic effects arising from temperature-induced fluctuations of the internal fields, resulting from motions of the molecular skeleton onto which muonium is stuck will lead to a reduction of the second moment through averaging of the local dipolar field due to the modulation of the dipole-dipole interactions [34]. Explicit expressions to carry out such calculations obviously require the specification of some dynamical model to represent the molecular motion and in most cases lead to rather cumbersome formulae the evaluation of which can only be performed by numerical means. Most practical situations however base their interpretation of results concerning the variation of second moment with the correlation time of the underlying motion on the basis of the classic Kubo and Tomita [35] formulation of motional narrowing which, under the assumption of the validity of the fast-fluctuation limit leads to simplified

expressions for the relaxation rate which is now given by,

$$\lambda_{TF} = -\gamma_{\mu}^{2} M_2 \tau_c \tag{3}$$

where τ_c stands for the correlation time of the fluctuating fields. With values at hand we can now evaluate the order of magnitude of dynamic phenomena being sampled at the experiment. Lets first take the value for M_2 derived the calculation just referred to above as well as that resulting from NMR measurements [17]. Once plugged into the above equation and consideration of the order of magnitude of the relaxation rates it yields estimates for the correlation time for temperatures below the transition, that is below some 200 K of the order of $10^{-7}\mathrm{s}^{-1} - 10^{-6}\mathrm{s}^{-1}$ depending upon the value for the second moment taken for the calculation.

Above some 200 K the relaxation rate displayed in Fig.3 rapidly decreases with increasing temperature which, assuming the validity of Eq.3 within this range of temperatures, can be seen as a result of a concomitant reduction of the correlation time. The TF relaxation amplitude also displays a sudden jump at basically the same temperature as the relaxation rate does. The microscopic origin of such a steep step cannot be ascertained in full, but the data at hand suggests that well within the RP phase a free muon may combine with a nearly free rotating molecule to give rise to the diamagnetic 2-O-adamantane-Mu^{+} adduct or, as another possibility, a neutral 2-O-adamantane-Mu radical may capture a mobile free electron to give the diamagnetic 2-O-adamantane-Mu^{-} adduct.

To wrap up this section it seems pertinent to carry out an order of magnitude comparison of the results just described with those previously obtained by means of dielectric spectroscopy. To such an avail here we take the measured dielectric relaxation characteristic times [11] τ_d and consider them as time constants of some underlying orientational motions, an assumption here justifiable since we are only pursuing a comparison of the magnitude of transverse relaxation rates. Under such assumptions, closed form expressions for the relaxation rate due to purely dipolar interactions under the assumption of rotation Brownian motion, are given in the literature pertaining to plastic crystals [36] and may be adapted for the case of relaxation from unlike spins with the help of results given in Ref. [37]. The formula used for such a calculation yields,

$$\frac{1}{T_2^{calc}} = M_2 \times \left[4\tau_d + \frac{\tau_d}{1+(\omega_\mu - \omega_p)^2\tau_d^2} + \frac{3\tau_d}{1+\omega_\mu^2\tau_d^2} + \frac{6\tau_d}{1+\omega_\mu^2\tau_d^2} + \frac{6\tau_d}{1+(\omega_\mu + \omega_p)^2\tau_d^2} \right] \tag{4}$$

where M_2 stands for the *rigid lattice value* of the spectral second moment given by Eq.2, $\omega_{\mu,p}$ stand for the muon and proton Larmor frequencies for precession within a 50 G field and the τ_d are assigned to the three different sets of relaxation times reported in [11]. The results tell that the expected relaxation rates for the times corresponding to the main α and β relaxation processes detected within the SDP phases will be way out of the accessible window for μSR. A point of contact seems however to exist concerning rotational motions within the rotator phase where the calculated relaxation rates are within the interval $0.028\mu s^{-1} \leq \frac{1}{T_2^{calc}} \leq 0.010\mu s^{-1}$. The temperature dependence of such quantities is however Arrhenius-like which is in sharp contrast with the weak dependence observed for the relaxation rates above 220 K.

3.4 Measurements under Zero Field

As mentioned above, measurements were also carried out under zero applied field and varying temperature. The expectancy was that such measurements would encompass similar phenomena to those explored under TF as well as reveal some details pertaining the paramagnetic species which are to be expected. A detailed account of such measurements is given in the Supplementary Material section. The main findings which are shown in Figures S3 and S4 of such Material show that relaxation of the implanted muons towards thermal equilibrium proceeds following two steps with relatively well separated timescales. A fast process characterized by a rate λ_{ZF}^{f} is clearly visible for times below the first microsecond of the experimental histogram. The measured rates are about one order of magnitude larger than those sampled under TF conditions and their temperature dependence shown if Fig. S4 appears to follow the general trends explored under TF, namely a relatively smooth decrease with temperature up to some 170 K followed by an abrupt decrease and a rather soft temperature dependence above 220 K. The results are however qualitative since the time scales of such phenomena are close to the limit of instrumental observation. In contrast, the slowest relaxation process named as λ_{ZF}^{s} could be followed

in more detail. The data of Fig. S4 nicely follows the same trend explored under TF and its general shape could also accounted following the same steps described to parametrize the data given in the next section.

Data concerning the temperature dependence of the fractional amplitude displayed in Fig. S4 of the Supplementary Material section show some significant difference with respect to those plotted in Fig.3 at low temperatures although also shows a steep riseup at the phase transition which is taken as a signature of conversion processes leading to a dominant diamagnetic fraction.

4 Discussion

As known since the pioneering work of Adachi *et al.* [38], rapidly cooling some molecular crystals from their metastable rotator- or plastic-crystal phase can avoid the transition into their fully ordered ground states, driving those samples into some "glassy-crystal state", where translational order is preserved but the strong rotational disorder characteristic of the plastic-crystal phases is partially quenched. Substituted adamantane compounds such as 1-cyanoadamantane (CN-a, $C_{10}H_{15}CN$) were found to conform to such a category of materials and dynamic and thermodynamic properties were soon investigated [39–41]. The results showed the persistence of uniaxial reorientational motions well within the "glassy-crystal state". The material here investigated, which has some distinctive features with respect to CN-a, has shown the persistence of motions within its "glassy-crystal state" down to around 150 K, which are found to be fast enough to be explorable by means of dielectric broadband spectroscopy [11]. The thermal and dynamic characterization of such a metastable phase, as well as the comparison of its properties to those of the true crystal ground state, namely an orthorhombic crystal with $Cmc2_1$ lattice structure, has recently been achieved [9,13]. Both crystals show a rather small difference in volume, which indicates that the transition into the truly ordered ground state involves a volume contraction, amounting a mere two per cent. In stark contrast, dynamical quantities such as the spectral frequency distribution, as well as the thermal conductivity of both phases, unveil significant differences attributable to substitutional disorder [13]. More specifically, the frequency distribution of the metastable phase shows a population of vibrational low energy states larger than that of the ground state, a difference most noticeable somewhat above 1 THz. Such frequencies which are found to correspond to well defined excitations of mostly librational character are strongly coupled to the acoustic modes [42,43] and become well resolved within the "glassy-crystal" as motions of molecules perpendicular to the molecular dipole axis. The results are also in agreement with previous results obtained from Raman spectroscopy reported by Bistricic *et al.* [17], who measured a well resolved, narrow band centered at some 1.1 THz, which shifts up to 1.26 THz in going down to the crystal ground state.

Structurewise, one expects the SDP phase of the material here under consideration to share some common features with the corresponding glassy phase of the cyano-substituted analogue, which shows strong diffuse scattering in the diffraction patterns attributed to the presence of antiferroelectric domains [44] having a coherence length up to 20 Å. The expectancy of strong antiferroelectric interactions as the relevant processes driving the order-disorder transitions in crystalline adamantanone stems from the rather large value of its molecular dipole moment, 3.4 Debye (1 Debye $\approx 3.335 \times 10^{-30}$ C. m), which compares with that of 3.83 Debye of CN-a. In fact, some hints of antiferroelectric behaviour can be inferred from its Kirkwood g_k factor which attains values well below 0.2 within the SDP and shows a sudden jump up to figures above 0.4 above some 200 K [11].

The experimental data for the relaxation rates can be well accounted for using a simple square-root law as previously applied to structural glasses that is [18,19], grounded on the kinetic theory of the glass transition [45,46] and should be valid for temperatures not too far below the glass-transition region,

$$\begin{aligned} \lambda_{TF} &= A\sqrt{|\,\frac{T-T_c}{T_c}\,|} + \xi(T), T \leq T_c \\ \lambda_{TF} &= \xi(T) = a + b\,|\,\frac{T-T_c}{T_c}\,|, T \geq T_c \end{aligned} \tag{5}$$

where a, b are parameters to account for the soft temperature dependence of data measured above the transition (i.e. above 220K). In the above formula, T_c stands for some critical temperature, A is a global scaling constant and $\xi(T)$ comprises a background term set by data measured above the transition.

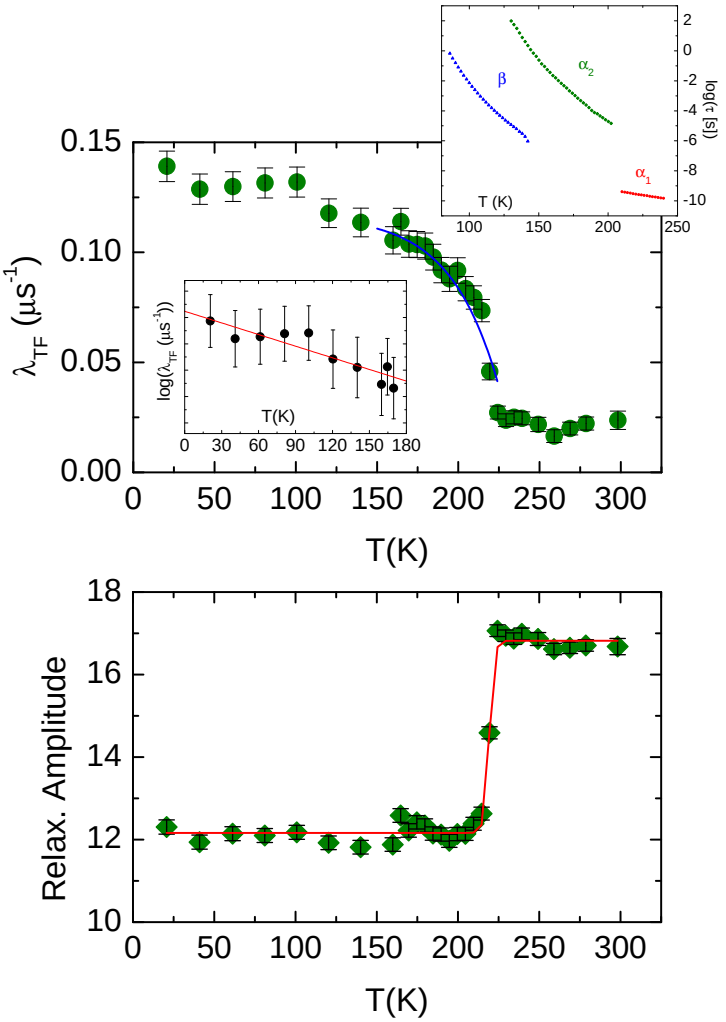

Figure 4: The upper frame depicts data for the relaxation rate as measured under transverse field. The red line that interpolates data for the lower temperatures depicts the single-exponential dependence referred to in the text. The blue line shows the best approximation achieved for data about the transition range in terms of the square-root singularity (see text). Best parameter values were $T_c = 220.5 \pm 9.27$ K, $A = 0.17 \pm 0.11\ \mu s^{-1}$, $a = 0.025 \pm 0.02\ \mu s^{-1}$ and $b = 0.083 \pm 0.04\ \mu s^{-1}$. The lower frame depicts the relaxation amplitude and the fit of a logistic function of the form $a_{TF}(T) = bcgr + ampl/(1 + \exp(-r(T - T_c))$, where r stands for the growth rate and T_c for some critical temperature (see text). The obtained values for the parameters are 12.16 ± 0.05 for the background term, 4.66 ± 0.09 for the amplitude, 220.5 ± 9.27 K for the critical temperature and 0.665 ± 0.18 for the r parameter. The upper inset shows the α and β relaxation times (in log scale) obtained from dielectric spectroscopy [11].

Figure 4 summarizes the main results of the data analysis followed here. Consideration is only made of the TF data, since it enables the analysis to be made of the diamagnetic species alone. In addition, rather than considering the relaxation rates alone, a joint analysis of the rates and the relaxation amplitudes was carried out. As stated above, data for the lower temperatures reasonably follow an exponential temperature dependence while the trend shown by data at temperatures approaching the known thermodynamic transition is found to be well approximated by Eqn.5. However, the temperature dependence of the relaxation amplitude departs from predictions made on kinetic theory grounds, which expect the relaxation amplitude to be proportional to $((T - T_c)/T_c)^{1/2}$ [45]. A number of reasons may account for such a discrepancy. In fact we expect that other processes than those of purely dynamic origin such as those related to muonium formation will contribute to the observed relaxation and these will yield a more complicated temperature dependence of the relaxation amplitudes. The temperature dependence

of such phenomena, which have to do with aspects of muonium chemistry, exhibits a remarkably abrupt jump which strongly suggests that they are strongly coupled to the underlying dynamics. On such grounds we carry out an analysis in empirical terms, fitting the data to the logistic function $(1 + \exp(-r(T - T_c))^{-1}$, as already done our previous studies on structural glasses. The derived value for $T_c = 220.5(1)$ K nicely matches that resulting from the analysis of the relaxation rates for the slow process measured under zero field (see Supplementary Material).

A comparison of the current results with those from earlier observations in structural glass$\longrightarrow$liquid [18,19] transitions seems in order. The main differences observed between the current data and those for structural glasses studied so far [18,19] concerns the steepness of the relaxation amplitude and relaxation rates when approaching the transition region, as well as the value of the critical temperature which here comes within the range of those corresponding to the observed thermodynamic transition whereas data for structural glasses point towards a value some tens of kelvins above the temperature signalling the upper range of the glass$\longrightarrow$liquid transitions. The smeared out nature of the transition in the amorphous materials if compared to the present results can be gauged from the value of the r parameter or growth rate, which comes to be one order of magnitude larger for our current sample than those values found for true glass-forming materials. In addition, it is worth pointing out that in contrast with previous studies on amorphous matter, the present results enable us the assignment of the degrees of freedom which become partially arrested at the RP$\longrightarrow$SDP phase change. In fact, on the grounds of previous results we can assign the observed dynamic phenomena to a change in molecular dynamics which passes from reorientations of the dipole axis along the six $< 001 >$ cubic lattice directions as well as $\pi/2$ rotations about the C=O axis within the RP crystal to just reorientational librations together with the three possible C=O directions related to the statistical occupancies of the Oxygen atom.

Although a detailed theory able to describe the muon relaxation rates across glass transitions is not yet available, here we have exploited the strikingly analogous behaviour exhibited by the Lamb-Mössbauer factor for recoilless emission f which can be directly related to microscopic quantities for which predictions made on the basis of the Mode/Coupling Theory for the glass transition have been developed [47]. Such an experimental observable was studied in detail for network and some metallic glasses [48, 49] by Mössbauer spectroscopy as well as in measurements based on the technique of nuclear resonant scattering of synchrotron radiation [49, 50]. The measured f factor is directly related to the mean-squared amplitudes of thermal vibration, namely $f = \exp -\frac{1}{3}Q^2\overline{u^2}$, where Q stands for the incident wavevector of the probe radiation and $\overline{u^2}$ is the atomic mean-square displacement which for temperatures well below any glass transformation is expected to follow the behaviour of a Debye solid and thus lnf should follow a linear decrease with increasing temperature. At temperatures approaching phase transformations it shows a stronger drop much alike those found in the present study. In fact, for temperatures approaching T_g, such studies show that strong anharmonic effects set in, leading to a strong increase in the atomic mean-square displacements and thus to a strong drop of f, as observed by experiment [51].

As known for long, muon spin spectroscopy is a privileged tool to explore or ratify some issues pertaining to the critical behaviour of a good number of systems, which in most cases concern magnetic systems, where the technique enables direct access to the order parameter such is the case for the internal field or sample magnetization. Some of the reported studies in glasses [52] typically monitor some single-particle property such as the variation with temperature of the hyperfine couplings of the muon adduct, which can be related to changes in molecular mobility setting in above the glass transition, leading to a reduction of the relaxation time or alternatively, in Fluorine-containing polymers [53], the variation with temperature of the dipolar frequency and relaxation rate of the F-Mu(+)-F state resulting from muon implantation. In contrast, the findings reported here display clear critical behavior features resulting from the rather strong coupling of the muoniated adduct to the lattice degrees of freedom. Our current results concerning the temperature dependence of the relaxation amplitude are somewhat reminiscent of the behaviour exhibited by some spin glasses [54], which display a sigmoid-like shape in the amplitude centered at temperatures somewhat above T_g and this was interpreted as evidence of the coexistence of islands of mobility above T_g with frozen impurity spins surrounded by areas exhibiting fast fluctuations. Such a similarity however contrasts with the rather different behaviour of the relaxation rates exhibited below and above the spin glass-transition, which usually shows a dependence of the kind $\lambda \propto [(T - T_g)/T_g]^{\gamma}$ with $\gamma < 1$. Also, some recent reports on the nature of order-disorder transitions on conventional ferroelectrics [55] are worth investigating and special attention may be paid to the finding

of short-lived local atomic configurations within the high temperature cubic phase, which develop within the electrically ordered phase well below the macroscopic transition temperature, as well as the converse that applies for the higher symmetry cubic phase below the transition.

The prediction of a sharp glass-transition at T_c is sometimes listed as one of the failures of the kinetic theory treatments of the glass-transition, usually called mode-coupling theories [56]. It is however worth remarking that, contrary to reported efforts on the quest for such dynamic singularity, often involving significant massaging of experimental data which are usually limited in frequency range, the appearance of critical features in the temperature dependence of the relaxation rates and amplitudes found in μSR studies provides a significant counterexample. The technique which genuinely probes single-particle dynamics is able to explore eight decades in frequency without requiring extensive data manipulation.

A thorough discussion on the meaning of T_c for a crystalline material such as ours is well beyond the scope of the present communication. The issue has been addressed in the past by theoretical [46] and computer simulation means [57, 58] and the matter has been rationalized using as a parameter the decreases with temperature of the lattice constants. Decreasing the temperature thus leads to an increasingly strong hindrance of the nearly freely reorienting molecules within the plastic crystalline RP state. The net effect of the lattice contraction when transit into the monoclinic crystal is completed will result in some orientational cage within which molecular orientations are captured on a certain timescale, and a only a small set of possible motions will be then allowed. The analogy with canonical liquid$\longrightarrow$glass transitions is given further support from thermal and dielectric spectroscopy results commented on above. The main difference of this study concerns the existence of a true structural transition which makes the observed temperature dependences of the relaxation rates better defined, that is less smeared out than those previously observed for amorphous matter.

5 Conclusion

The results reported here show that the crystal phase transition from the rotator phase into the substitutionally disordered phase retains characteristic phenomena usually found in liquid$\longrightarrow$glass transitions of structural glass-formers. Relatively fast and large-amplitude reorientations within the RP crystal get arrested below the transition, although dynamical processes within a region of nanoseconds to milliseconds continue to be thermally activated, as dielectric spectroscopy and the current results exemplify.

The present results, to the best of the authors knowledge, provide the first direct experimental evidence of the appearance of a typical glassy-dynamics singularity on a transition connecting two partially ordered crystal states. Previous results, mostly on purely theoretical [46], simulation [57] or somewhat mixed approaches [58] pointed towards the possible presence of such a singularity. Our results show that the techniques here employed may be profitably employed to carry out these kind of studies for a wide variety of samples to explore dynamical features for time scales unreachable by other more common experimental approaches. In contrast with other nuclear techniques, μSR allows a far simpler analysis of the measured data and does not require the use of any external probe.

Acknowledgements

This work was supported by the Spanish Ministry of Science and Innovation through projects FIS2014-54734-P and MAT2012-33633 and by the Generalitat de Catalunya under project 2014 SGR-581.

References

[1] J. Ichikawa, N. Hoshino, T. Takeda, T. Akutagawa, J.Am.Chem.Soc.**137**, 13155 (2015).

[2] For a recent appraisal of theoretical efforts pertaining glass-transitions see for instance L.M.C. Janssen *et al.* J.Stat.Mech.:Theory and Exper. **2016**, 054049 (2016); J.S. Langer Rep.Prog.Phys. **77**, 042501 (2014); S. Kasmakar *et al.* Rep.Prog.Phys. **79**, 016601. For recent experiments suggesting the existence of an underlying thermodynamic transition see S. Albert *et al.* Science **352**, 1308 (2016).

[3] M. Gomez, S.P. Bowen, J.A. Krumhansl, Phys.Rev. **153**, 1009 (1967).

[4] E. Grannan, M. Randeria, J.P. Sethna, Phys.Rev. **B 41**, 7784 (1990).

[5] F. Ritort, P. Sollich, Adv.Phys. **52**, 219 (2003).

[6] M. Jimenez-Ruiz, *et al.* Phys.Rev.Lett. **83**, 2757 (1999).

[7] A. Criado *et al.* Phys.Rev. **B 61**, 12082 (2000); M.A. Ramos *et al.* Phys.Rev.Lett. **78**, 82 (1997).

[8] G. Remenyi *et al.*, Phys. Rev. Lett. **114**, 195502 (2015).

[9] P. Negrier *et al.*, Cryst.Growth.Des. **14**, 2626 (2014).

[10] R. Brand, P. Lunkenheimer and A. Loidl J. Chem. Phys. **116**, 10386 (2002).

[11] M. Romanini *et al.* Phys.Rev. **B 85**, 134201 (2012).

[12] A.I. Krivchikov, G.A. Vdovichenko, O.A. Korolyuk, F.J. Bermejo, L.C. Pardo, J.Ll. Tamarit, A. Jezowski, D. Szewczyk, J. Non-Cryst. Solids **407**, 141 (2015).

[13] D. Szewczyk *et al.*, J.Phys.Chem.B **119** , 8468 (2015).

[14] X. Tang, A.J. Benesi, J.Phys.Chem. **98**, 2844 (1994).

[15] B. Ben Hassine, Ph. Negrier, M. Romanini, M. Barrio, R. Macovez, A. Kallel, D. Mondieig and J. Ll. Tamarit Phys.Chem.Chem.Phys. **18**, 10924 (2016).

[16] J. C. Martinez-Garcia, J. Ll. Tamarit, S. Capaccioli, M. Barrio, N. Veglio, and L. C. Pardo, J. Chem. Phys. **132**, 164516 (2010).

[17] R. Decressain, J.P. Amoreux, E.Cochon, Phys.Status Solidi **190**, 295 (1995); J.P. Amoreux, M. Castelain, M. Bee, B. Arnaud, M.L. Shouteeten, J.Phys.C:Solid State Phys. **15**, 1319 (1982); P.D. Harvey, I.S. Butler, D.F.R.Gibson, P.T.T. Wong, J.Phys.Chem.**90**, 4546 (1986); L.Bistricic, G. Baranovic, V. Volovsek, J.mol.struc. **482-483**, 79 (2002); L. Bistricicik, L.Pejon, G.Baranovic, J.Mol.Struc. **594**, 79 (2002).

[18] F. J. Bermejo, I. Bustinduy, M. A. Gonzalez, S. H. Chong, C. Cabrillo, S. F. J. Cox, Phys. Rev. **B 70**, 214202 (2004).

[19] C. Cabrillo, F. J. Bermejo, S. F. J. Cox, Phys. Rev. **B 67**, 184201 (2003).

[20] F. L. Pratt, Physica B **289-290**, 710 (2000); software available to download from http://www.isis.stfc.ac.uk/groups/muons/downloads/

[21] O. Arnold, J.C. Bilheux, J.M. Borreguero *et al*, Nucl. Instr. Meth. A **764**, 156 (2014); software available to download from http://www.mantidproject.org.

[22] In what follows we will adhere of the standard practice of naming muonium as Mu to the bound state of an incoming muon and an electron, while the symbol μ^+ is here restricted to denote the pre-thermalized, incoming muons. In turn, atomic muonium within the sample is named as Mu$^{\cdot}$ and Mu$^+$ will stand for muons within some cationic state with the host molecule. Thus notice that when referring to Mu within a chemical formula this will represent muonium covalently bonded through O-Mu σ bonds.

[23] P. Verma, A. Perera, J.A. Morales, J.Chem.Phys. **139** 174103 (2013).

[24] P.J. Krusic, T.A. Rettig, P.v.R. Schleyer, J.Am.Chem.Soc. **94** 995, (1972).

[25] S. J. Clark, M. D. Segall, C. J. Pickard, P. J. Hasnip, M. J. Probert, K. Refson, M. C. Payne , Zeitschrift fuer Kristallographie **220**, 567 (2005).

[26] K. Aidas *et al.* WIREs Comput. Mol. Sci. **4** 269, (2014) (doi: 10.1002/wcms.1172); Dalton, a molecular electronic structure program, Release Dalton2016 (2015), see http://daltonprogram.org.

[27] Calculations carried out at Hartee-Fock level yield energy differences of 4.085 eV and 4.102 eV depending upon the chosen basis which were taken as 6-31G and cc-pVTZ respectively. DFT results using the B3LYP hybrid functional yielded results of 4.580 eV and 4.749 eV respectively. In all cases the neutral muoniated radical appears as the most stable.

[28] S.F.J. Cox, M.C.R. Symons, Radiat.Phys.Chem. **27**, 53 (1986); E. Roduner, Radiat.Phys.Chem. **28**, 75 (1986); A. Hill *et al.* J. Chem. Soc. Faraday Trans. **1**, 433 (1984).

[29] C.P. Slichter, *Principles of Magnetic Resonance*, 3rd Ed. SpringerVerlag Series in Solid State Sciences 1, Berlin, 1990, p. 84. A detailed account of a calculation of motional effects on the second moment can be found in R. Goc, Z. Naturforsch. **57a**, 29 (2002)

[30] P. Mendels in http://www.isis.stfc.ac.uk/groups/muons/muon-training-school/2014-mendels-nmr14921.pdf.

[31] R. Goc, Comp. Phys. Comm. **162**, 102 (2004).

[32] J.H. Van Vleck, Phys. Rev. **74**, 1168 (1948).

[33] A. Schenk, *Muon Spin Rotation Spectroscopy. Principles and Applications in Solid State Physics*, Adam Hilger Ltd., Bristol 1985, p. 47.

[34] In analogy with NMR, thermal motions with some frequency ω_m modulate the dipole-dipole interaction, averaging its static part and giving rise to satellite lines shifted at side frequencies $2\pi\omega_m$ with respect to the Larmor frequency. The net result of such averaging is to narrow the central part of the spectrum and leads to the expectancy of broad wings corresponding to series of shifted satellite lines which usually are too weak to be observable. The second moment of the central part of the spectrum will then become smaller than its rigid lattice value. It could however equate such value if the contribution from the sidebands were included in the relevant integral. As examples see L. Latanowicz, E.R. Andrew, E.C. Reynhardt, J.Magn.Res. **107**, 194 (1994); E.R Andrew, J. Lipofsky, J. Magn.Res. **8**, 217 (1972).

[35] R. Kubo, K. Tomita, J.Phys.Soc.Japan, **9**, 888 (1954).

[36] J.N. Sherwood *The Plastically Crystalline State (Orientationally Disordered Crystals)*, Wiley, N. Y. 1979, p.162.

[37] J. McConell *The Theory of nuclear magnetic relaxation in liquids*, Cambridge Univ. Press. 1987 p.91.

[38] K. Adachi, H Suga, S. Seki, , Bull.Chem.Soc. Japan **41**, 1073 (1968).

[39] M. Bee, M. Foulon, J.P. Amoreux C. Caucheteux, C. Poinsingnon, J.Phys. C: Solid State **20**, 337 (1987) and references therein.

[40] K. Pathmanathan, G.P. Johari, J.Phys.C:Solid State Phys. **18**, 6635 (1985).

[41] S.A. Lusceac *et al.*, J.Chem.Phys. **121**, 4770 (2004) ; S. Lusceac, J. Gmeiner, E.A. Rössler, J.Chem.Phys. **126**, 014701 (2007).

[42] J. Lefebvre, J.P. Rolland, J.L. Sauvajol, B. Hennion, J.Phys.C: Solid State **18**, 241 (1985); J.L. Sauvajol, J. Lefebvre, J.P. Amoreux, M. Bee, J.Phys.C: Solid State **15**, 6523 (1982).

[43] Calculations of phonon dispersion curves as well as their associated character have ben carried out using the CASTEP code and are available upon request.

[44] M. Descamps C. Caucheteaux, G. Oudou and J.L. Sauvajol, J. Physique Lett. **45**, L-719, (1984).

[45] W. Götze, Z.Phys. B **60**, 195 (1985); J. Thakur and J. Bosse, Phys.Rev.A **43**, 4378 (1991).

[46] M.Ricker, R.Schilling, Phys.Rev.E **72**, 011508 (2005); M.Letz, R. Schilling, A.Latz, Phys.Rev.E, **62**, 5173 (2000); C. DeMichele,R. Schilling, F. Sciortino, Phys.Rev.Lett. **98**, 265702, (2007)

[47] W. Götze, in Liquids, freezing and glass transition, Part I, p. 287, J.P. Hansen, D. Levesque, J. Zinn-Justin (Eds.), Les Houches Session LI, North Holland, Amsterdam 1991.

[48] See for instance P.M. Boolchand in *Insulating and semiconducting glasses*, P. Boolchand (Ed.), chapt. 6B, p 369 World Scientific, Singapore 2000; and P. Boolchand *et al.* Solid State Ionics, **39**, 81 (1990).

[49] A. Meyer, H. Franz,B. Sepiol, J. Wuttke, W. Petry, Europhys.Lett. **36**, 379 (1996).

[50] I. Sergueev *et al.* Phys.Rev. B **66**, 184210 (2002); A. Meyer *at al.* Z.Phys.B **103**, 479 (1997).

[51] W. Dorster, S. Cusack, W. Petry, Nature **337**, 754 (1989).

[52] F.L. Pratt *et al.*, Phys.Rev. B **72**, 121401(R) (2005).

[53] I.McKenzie *et al*, Phys.Rev.E **89**, 022605 (2014).

[54] See for instance C. Boekema *et al.*, Hyperf.Interact. **31**, 369 (1986), and Ref. [33] p. 200.

[55] H. Fang, Y. W. Wang, S. Shang, Z.K. Liu, Phys.Rev. **91**, 024104 (2015).

[56] D.R. Reichman, P. Charbonneau,J.Stat.Mech.:Theory and Exper. P05013 (2005).

[57] M. Ricker, F. Affouard, R. Schilling and M. Descamps, J.Non-cryst.Solids **352**, 4814 (2006).

[58] F. Affouard, M. Descamps, Phys. Rev. E **72**, 012501 (2005).